JOURNAL OF MATERIALS SCIENCE 28 (1993) 5534–5539

# Phase boundary of an LMN–PZ–PT three-component system

JIN-CHEN SHAW, KUO-SHUNG LIU, I-NAN LIN*
*Department of Materials Science, and *Materials Science Centre, National Tsing Hua University, Hsin-Chu, Taiwan*

Piezoelectric ceramics of $Pb(Zr,Ti)O_3$ (PZT) were added to a third component $La(Mg_{2/3}Nb_{1/3})O_3$ (LMN) to form an LMN–PZ–PT three-component system. The morphotropic phase boundary (between the tetragonal phase and rhombohedral phase) was close to the $PbZrO_3$ site. The phase boundary between the tetragonal and cubic phase was close to the $PbTiO_3$ site, and the composition 9/62/29 was the three-phase point. The grain size could be reduced by increasing the amount of LMN in the PZT system. Replacing lead ions with lanthanum ions would induce a strain in the lattice because the diameter of the lanthanum ion is smaller than that of the lead ion. The best electromechanical coupling coefficient ($K_p$) found was 53.7 and the component was close to the morphotropic phase boundary.

## 1. Introduction

The ferroelectric ceramics $Pb(Zr,Ti)O_3$ (PZT) is a solid solution of lead zirconate and lead titanate. It has a perovskite-type structure and is a basic piezoelectric material. Piezoelectric transducers and pyroelectric detectors have important technological applications [1, 2]. The naturally high dielectric constant of PMN makes it a very promising material for ceramic capacitors. The large electrostrictive strain accompanying the high dielectric constant also makes it important in application for electrostrictive devices such as actuators [3–5].

PZT is also an important material for electro-optic applications, when doped with lanthanum to form PLZT [6, 7]. PMN doped with lanthanum to form PLMN also exhibits electro-optic properties [8]. PZT when added to $La(Mg_{2/3}Nb_{1/3})O_3$ (LMN) forms LMN–PZ–PT which is also interesting because it may exhibit all these properties: dielectric constant, piezoelectric and electro-optic properties.

The best piezoelectric properties of PZT exist in the phase boundary between the tetragonal and rhombohedral phases, known as the morphotropic phase boundary (MPB) [9, 10]. Therefore, a study of the microstructure and piezoelectric properties of the morphotropic phase boundary and the tetragonal–cubic phase boundary was undertaken.

## 2. Experimental procedure

### 2.1. Composition selection

The compositions selected for the present study were of the type $x$LMN–$y$PZ–$z$PT, where $x + y + z = 1$, with $x$ varying between 3 and 15 in steps of 3. The $y/z$ ratio was close to the tetragonal–rhombohedral phase and tetragonal–cubic phase boundaries.

### 2.2. Ceramic sample preparation

The ceramic samples of the LMN–PZ–PT composition were prepared by the mixed oxides methods. The starting materials consisted of high purity PbO, $ZrO_2$, $TiO_2$, $La_2O_3$, MgO and $Nb_2O_5$ in the correct composition. The weights of the fine oxides were determined from the molar composition, and the oxides were then wet ball milled in ethanol for 8 h. The mixed powder was then dried and calcined at 850 °C in covered alumina crucibles for 6 h. The calcined powders were then wet ball milled in ethanol with the addition of 0.5 wt % PVA for 8 h, dried and pulverized. The fine powders were formed into a 12 mm diameter and 1–2 mm thick pellets using a pressure of 1000 kg cm$^{-2}$.

The pellets were then sintered at 1250 °C for 1 h in sealed alumina crucibles. A PbO-rich atmosphere was maintained by placing $PbZrO_3$ inside the crucible in order to compensate for the PbO weight loss. Silver paint was applied by firing onto the fine polished surfaces of the sintered pellets at 580 °C for 1 h. All the sintered samples were then poled in silicone oil at 120 °C for 20 min under a d.c. field of 3 kV cm$^{-1}$. Poled samples were aged for 24 h prior to property measurement.

### 2.3. Measurement

#### *2.3.1. Structure measurement*

All the sintered samples were analysed with an X-ray diffractometer (Rigaku DMAX-II) to identify their phases at room temperature, using Cu$K_\alpha$ radiation.

#### *2.3.2. Field-induced polarization*

The polarization versus electric field hysteresis loop was studied at room temperature, and at alternate



0022–2461 

field levels at 60 Hz using a modified Sawyer-Tower circuit [11].

### 2.3.3. Piezoelectric properties

The electromechanical coupling coefficient, $K_p$, and mechanical quality factor, $Q_m$, were calculated from

$$K_p^2 = [2.51(f_a - f_r)/f_r]^{1/2} \quad (1)$$

and

$$Q_m = [4\pi(f_a - f_r)RC]^{-1} \quad (2)$$

The resonant, $f_r$, and antiresonant, $f_a$, frequencies of the fundamental modes of the disc-samples were measured using an HP4194 impedance analyser.

## 3. Results and discussion

### 3.1. Crystal structure

The phase boundary between the tetragonal and rhombohedral phase was at a Zr/Ti ratio of 52/48 for PZT piezoelectric ceramics. An addition of 3, 6, 9, 12 and 15 mol% $La(Mg_{2/3}Nb_{1/3})O_3$ from the phase boundary of the LMN–PZ–PT three-component system could be determined from the X-ray diffraction pattern, as shown in Fig. 1. The crystal structure was tetragonal when the diffraction pattern had both (0 0 2) and (2 0 0) X-ray peaks; but it may be rhombohedral or cubic if the diffraction pattern only contains a (2 0 0) peak.

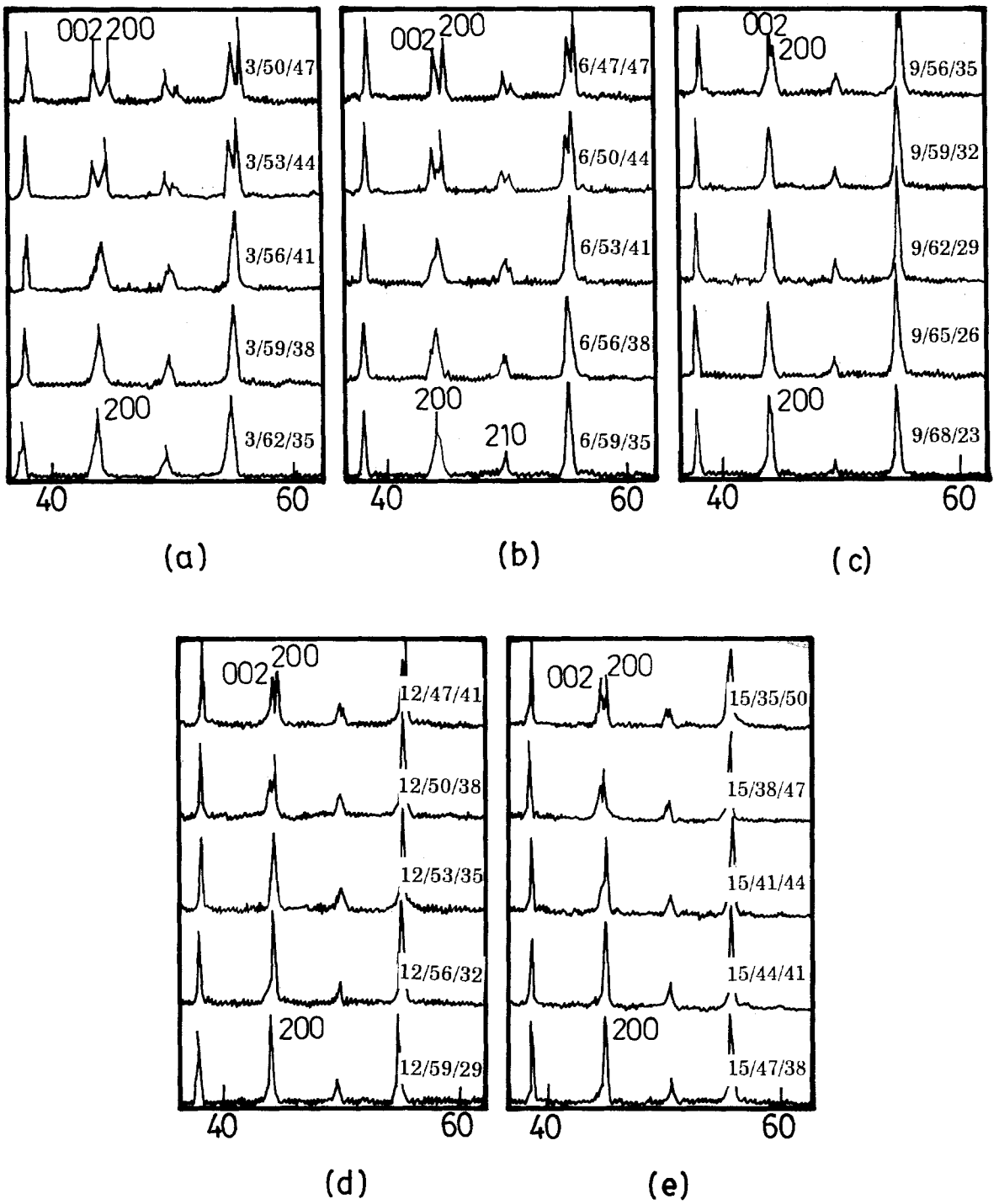


*Figure 1* The X-ray diffraction patterns of $x$LMN–$(1-x)$ PZT: (a) $x = 3$, (b) $x = 6$, (c) $x = 9$, (d) $x = 12$, (e) $x = 15$ close to the phase boundary.

The phase boundaries were, respectively, between 3/56/41 and 3/53/44, 6/56/38 and 6/59/35, 9/62/29 and 9/59/32, 12/53/35 and 12/50/38, 15/41/44 and 15/38/47, when 3, 6, 9, 12 and 15 mol % LMN was added to the PZT system (Fig. 1).

The lattice parameter, measured from the X-ray diffraction pattern, could be used to calculate the unit cell volume. The relationship of unit cell volume to the Zr/Ti ratio is shown in Fig. 2. The unit cell volume increased with addition of LMN up to 9 mol %, and then decreased with further addition of LMN.

### 3.2. *P–E* hysteresis loop

Rhombohedral and cubic phases have almost the same crystal structure when the distortion angle is very small, therefore distinguishing between the rhombohedral phase and cubic phase (through use of an X-ray diffraction pattern) would be very difficult. The ferroelectric ceramics is a perovskite ($ABO_3$) structure which may be described as a simple cubic unit cell with a larger cation (A) on the corner, a small cation (B) in the body centre, and oxygens (O) in the centre of the faces. The B cation for ferroelectric ceramics will not be in the centre of the cubic unit cell. Therefore, this non-symmetrical centre will produce a dipole moment, which will line up for all unit cells when an electric field is applied. This dipole moment would produce a polarization which varies with changes in the electric field.

The rhombohedral phase belongs to ferroelectric ceramics and has a non-symmetrical centre. The polarization versus electric field plot would then have a hysteresis loop. On the other hand, the cubic phase which has a symmetrical structure, does not contain a dipole moment; the polarization versus electric field plot in this case does not have a hysteresis loop. To distinguish between rhombohedral and cubic phase crystal structure would be easier from the *P–E* curves.

The relationship between the polarization and electric field for the LMN–PZ–PT three-component system is shown in Fig. 3. All samples with 3, 6 and 9 mol % LMN added were ferroelectrics ceramics because they exhibited hysteresis loops. Both the tetragonal and rhombohedral phases were ferroelectric ceramics and had hysteresis loops, so that the structure transformed from the tetragonal phase to the rhombohedral phase when the Zr/Ti ratio was increased. The relationship between polarization and electric field was linear and the *P–E* curve did not exhibit a hysteresis loop when the Zr/Ti ratio was larger than 1.51 (for 88PZT–12LMN) and 0.93 (for 85PZT–15LMN); therefore, we know that the crystal structure transformed from the tetragonal phase to the cubic phase when the Zr/Ti ratio increased. A partial phase diagram of the LMN–PZ–PT system is shown in Fig. 4. The phase boundary of the tetragonal and rhombohedral phases was close to $PbZrO_3$ and the phase boundary of the tetragonal and cubic was close to $PbTiO_3$. The composition of the three-phase point was 9/62/29 in an LMN–PZ–PT three-component system.

### 3.3. Microstructure

The microstructure of the LMN–PZ–PT system is shown in Fig. 5. The grain size decreased when the amount of LMN added to PZT was increased. The structure of the PZT is perovskite ($ABO_3$) and the A and O ions form the face centre cubic. The volume of the unit cell is therefore determined by the diameter of the A and O ions.

Some lanthanum ions will replace lead ions when LMN is added to the PZT ceramics system, and the unit cell volume would therefore be decreased (Fig. 2) because the diameter of the lanthanum ion (0.114 nm) is smaller than that of the lead ion (0.12 nm). The

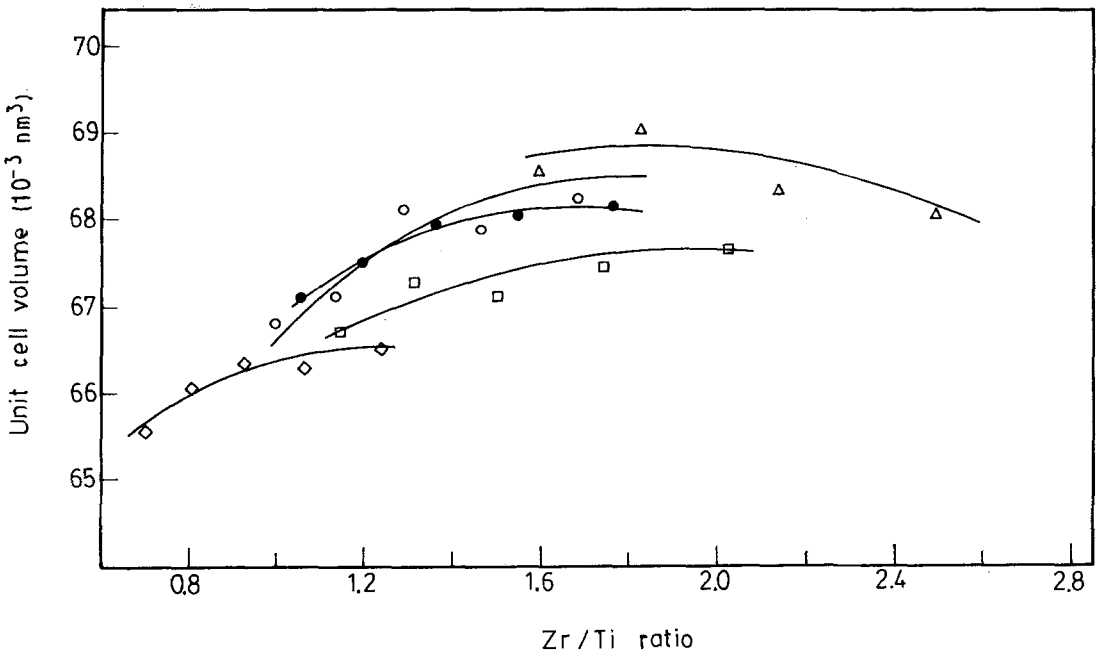


*Figure 2* The relationship between unit cell volume and Zr/Ti ratio with variation of LMN content: (●) 3%, (○) 6%, (△) 9%, (□) 12%, (◇) 15%.

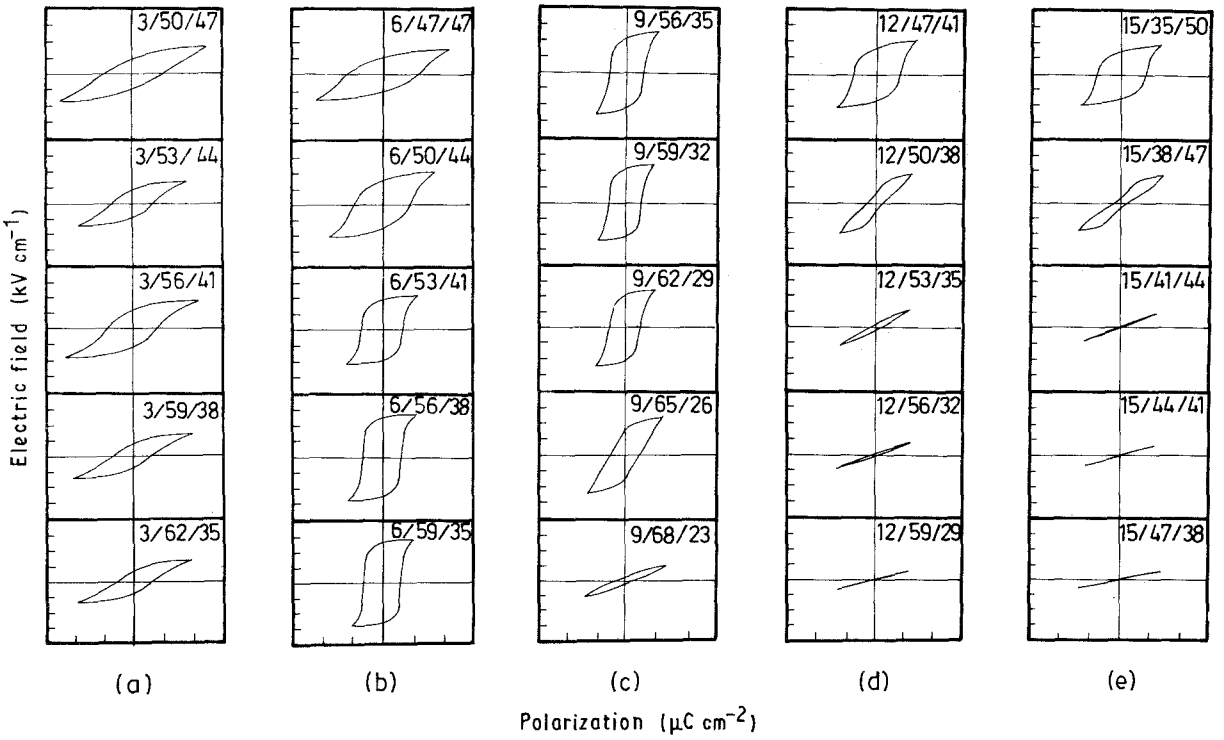


*Figure 3* $P$–$E$ curves for $x$LMN–(1 − $x$) PZT: (a) $x$ = 3, (b) $x$ = 6, (c) $x$ = 9, (d) $x$ = 12, (e) $x$ = 15 close to the phase boundary.

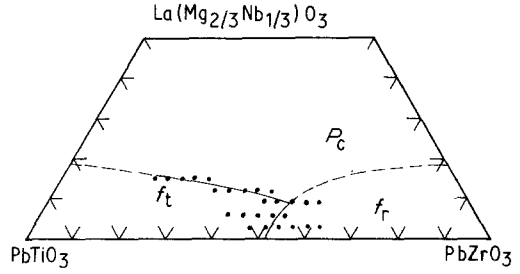


*Figure 4* The partial phase diagram of the LMN–PZ–PT three-component system.

reduction of the lattice parameter would induce some stress due to the occupation of A sites by lead ions. This stress will prevent the grain boundary from moving during the sintering process; therefore, the grain size would be reduced when the amount of LMN was increased.

Secondary recrystallization and growth occurred, so the grain size increased with 3 and 6 mol % LMN addition in the PZT ceramics system.

## 3.4. Piezoelectric properties

### *3.4.1. Coercivity ($E_c$)*

The coercivity of the LMN–PZ–PT system decreased when the Zr/Ti ratio was increased, as shown in Fig. 6a. The coercivities of the rhombohedral and cubic phase were smaller than that of the tetragonal phase. When the Zr/Ti ratio increased, the phase transformed from tetragonal to rhombohedral or cubic, which caused the coercivity to decrease. In addition, when the amount of LMN addition increased, the crystal structure would be closer to cubic, which also made the coercivity decrease.

### *3.4.2. Remanent polarization*

The polarization vector of the rhombohedral phase was ⟨1 1 1⟩. They had eight directions for dipole moment reorientation. The polarization vector of the tetragonal phase was ⟨0 0 1⟩. They had six directions for dipole moment reorientation. At the morphotropic phase boundary (MPB) there are fourteen directions for dipole moment reorientation due to the coexistence of rhombohedral and tetragonal phases [12, 13]. The dipole moment in the MPB could then reorientate itself more completely than the tetragonal or rhombohedral phase. The remanent polarization in the MPB was then also larger than that of the tetragonal or rhombohedral phase. The remanent polarization had a maximum at the morphotropic phase boundary when 3 and 6 mol % LMN was added to the PZT ceramics system, as shown in Fig. 6b. Because the cubic phase did not belong to the ferroelectric ceramics and the crystal structure was closer to cubic when the Zr/Ti ratio was increased at 12 and 15 mol % LMN addition, the polarization decreased with increasing Zr/Ti ratio.

### *3.4.3. Electromechanical coupling coefficient ($K_p$)*

The electromechanical coupling coefficient increased with addition of up to 6 mol % LMN and then decreased with further addition (Fig. 7a). The composition for the best $K_p$ was 6/53/41 when the value of $K_p$ was 53.7%.

### *3.4.4. Mechanical quality factor ($Q_m$)*

The mechanical quality factor decreased with increasing LMN content. The best $Q_m$ was 187 and could be achieved at the composition of 3/56/41.

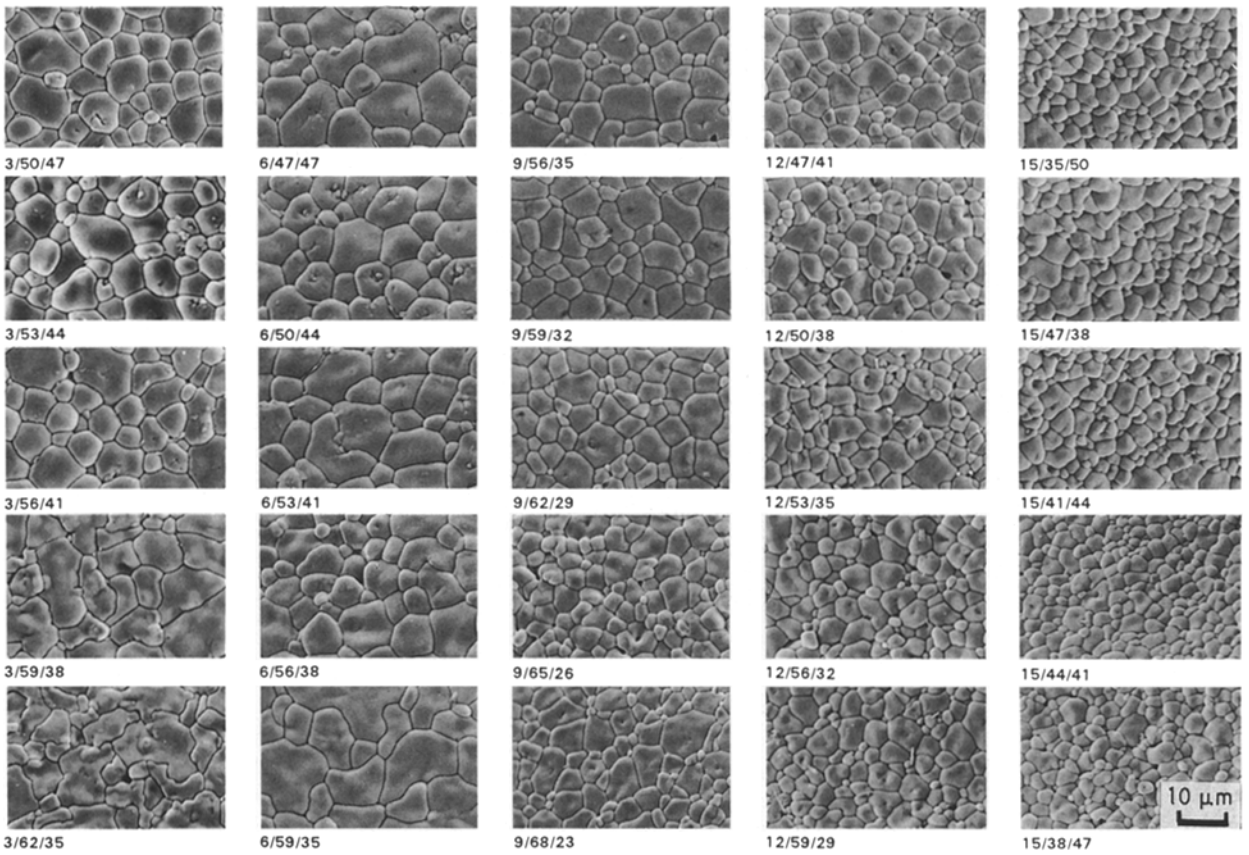


*Figure 5* The microstructure of $x$LMN–(1 − $x$) PZT: (a) $x$ = 3, (b) $x$ = 6, (c) $x$ = 9, (d) $x$ = 12, (e) $x$ = 15 close to the phase boundary.

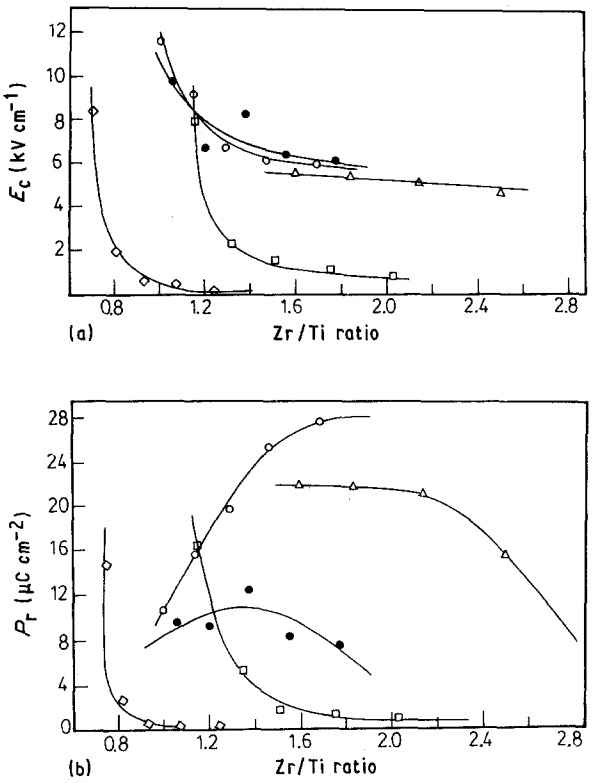


*Figure 6* The relationship of Zr/Ti ratio and (a) $E_c$, and (b) $P_r$ for various LMN contents: (●) 3%, (○) 6%, (△) 9%, (□) 12%, (◇) 15%.

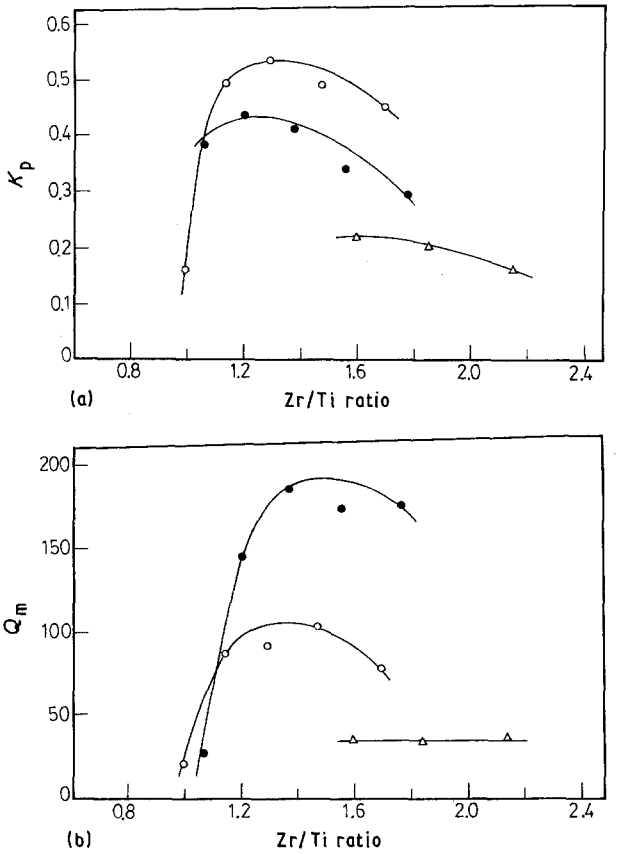


*Figure 7* The relationship of Zr/Ti ratio with (a) $K_p$, and (b) $Q_m$ for various LMN contents: (●) 3%, (○) 6%, (△) 9%.

## 4. Conclusions

1. When a third component, $La(Mg_{2/3}Nb_{1/3})O_3$, was added to $Pb(Zr,Ti)O_3$, a solid solution could form. The phase boundary existing between the tetragonal and rhombohedral phases was close to $PbZrO_3$; the tetragonal and cubic phase boundary was close to $PbTiO_3$; and the composition 9/62/29 was the three-phase point.

2. The diameter of the lanthanum ion (0.114 nm) is smaller than that of the lead ion (0.12 nm), therefore the unit cell volume and grain size would be reduced when lead ions were replaced by lanthanum ions.

3. The cubic structure did not have a non-symmetrical centre. A $P$–$E$ curve was therefore used to distinguish between the rhombohedral and cubic phase more easily than using the X-ray diffraction method.

4. The best electromechanical coupling coefficient found was 53.7% at a composition of 6/53/41. The 3/56/41 composition exhibited an efficient mechanical quality factor in the LMN–PZT piezoelectric ceramic system.

## Acknowledgement

We thank the National Science Council, Taiwan, for the financial support of this research under Grant NSC81-0404-E007-103.

## References

1. A. KUMADA, *Jpn J. Appl. Phys.* **24** (1985) 739.
2. K. UCHINO, *Bull. Amer. Ceram. Soc.* **65** (1986) 647.
3. S. NORMURA and K. UCHINO, *Ferroelectrics* **41** (1982) 117.
4. L. E. CROSS, S. J. JANG, R. E. NEWNHAM, S. NORMURA and K. UCHINO, *ibid.* **41** (1980) 117.
5. K. UCHINO, *Amer. Ceram. Soc. Bull.* **65** (1986) 647.
6. R. H. DUNGAN and G. S. SNOW, *J. Amer. Ceram. Soc.* **56** (1977) 781.
7. G. H. HEARTLING and C. E. LAND, *Ferroelectrics* **3** (1972) 269.
8. NAMCHUL KIM, DEAN A. McHENRY, SEI-JOO JANG and THOMAS R. SHROUT, *J. Amer. Ceram. Soc.* **73** (1990) 923.
9. S. STOTZ, *Ferroelectrics* **76** (1987) 123.
10. A. V. TURIK, M. F. KUPRIYANOV, E. N. SIDORENKO and S. M. ZAITSEV, *Sov. Phys. Tech. Phys.* **25** (1987) 1251.
11. J. K. SINHA, *J. Sci. Instrum.* **42** (1965) 696.
12. M. J. HAUN, E. FURMAN, S. J. JANG and L. E. CROSS, *Ferroelectrics* **99** (1989) 13.
13. YA. KVAPULIN'SKI, Z. SUROV'YAK, M. F. KUPRIYANOV, S. M. ZAITSEV, A. YA. DANTSIGER and E. G. FESENKO, *Sov. Phys. Tech. Phys.* **24** (1979) 621.

*Received 22 May*
*and accepted 15 June 1992*